Molecular and Magnetic Structure of the Paramagnetic Ion Pair Bis(tetraglyme)rubidium Biphenyl, $Rb^+[CH_3O(CH_2CH_2O)_4CH_3]_2C_{12}H_{10}^-$

J. J. Mooij, A. A. K. Klaassen, E. de Boer,*
H. M. L. Degens, Th. E. M. van den Hark, and J. H. Noordik

Contribution from the Research Institute for Materials (RIM), University of Nijmegen, Toernooiveld, Nijmegen, The Netherlands. *Received June 6, 1975*

Abstract: Single crystals of the paramagnetic ion pair bis(tetraglyme)rubidium biphenyl, $Rb^+[CH_3O(CH_2CH_2O)_4CH_3]_2C_{12}H_{10}^-$, have been synthesized. The crystal structure was determined at 100 K from three-dimensional x-ray data collected by counter methods. The crystals belong to the space group $C2/c$ with a = 30.68 (2), b = 9.79 (1), c = 23.71 (2) Å, β = 103.34 (6)°, Z = 8, and d_x = 1.31 g/cm^3. Each rubidium ion is spherically surrounded by ten oxygen atoms of the solvent molecules, leading to a solvent-separated ion-pair structure. The phenyl rings of the biphenyl anion have a dihedral angle of 9.4°. The magnetic properties have been investigated by means of ESR, NMR, and the foner vibrating sample magnetometer. It is shown that the results of both the paramagnetic susceptibility and the angular-dependent line width variation of the exchange-narrowed ESR line are consistent with the observed dimeric structure of the biphenyl anions. The susceptibility data and the temperature-dependent line width measurements indicate an exchange coupling in the dimer with a singlet ground state separated from the higher triplet state by $2J$ = 16.7 cm^{-1}.

During the last decades much work has been carried out on the negative ions of aromatic hydrocarbons, prepared by reduction of the neutral molecules with alkali metals.[1] Especially ESR and NMR experiments have provided much information on the structure of the alkali radical ion pairs in solution. Based on these experiments, two different types of ion pairs have been distinguished, namely "tight" or "contact" ion pairs and "loose" or "solvent separated" ion pairs.[1] To shed more light on the structure of the ion pairs, it would be of interest to carry out experiments on single crystals of the ion pairs. In 1970 Canters et al.[2] reported the first successful preparation of single crystals of the paramagnetic ion pairs of alkali biphenyl. A few years later Brooks et al.[3] published the crystal structures of some diamagnetic ion pairs, namely, triphenylmethyllithium tetramethylethylenediamine, fluorenyllithium bisquinuclidine, and the bis[(tetramethylethylenediamine)lithium] naphthalene dianion. In all these complexes, the lithium ion is directly coordinated to the aromatic moiety and from the outside coordinated to the nitrogen atoms of the solvent molecule, so that these complexes belong to the category of "contact" ion pairs. Recently the crystal structure of the potassium salt of 1,3,5,7-tetramethylcyclooctatetraene dianion has been published by Goldberg et al.[4] Noordik et al.[5] have published the crystal structures of the potassium and rubidium salts of the dianion of unsubstituted cyclooctatetraene (COT). All these crystals contained molecules of the solvent, diglyme ($CH_3O(CH_2CH_2O)_2CH_3$), from which the crystals were prepared. The crystal structures reveal that the alkali ions are located above the center of the planar eight-membered ring; the distances to the center of the ring are equal to the sum of the radius of the cation and the half thickness of the COT dianion. In the tetramethyl-substituted compound, the diglyme molecules are coordinated to the potassium ions through all three oxygen atoms; in the unsubstituted COT compounds, two different types of alkali ions can be discerned; one type is coordinated only by COT rings, whereas the other is coordinated on one side to the oxygen atoms of diglyme and on the other side by a COT ring. Therefore the single crystals of the alkali COT complexes can also be classified as contact ion pairs. It is interesting to note that Cox et al.[6] arrived at the same conclusion from NMR experiments on dipotassium cyclooctatetraene dissolved in diglyme.

In this paper we report the first crystal structure of a paramagnetic ion pair, viz., the rubidium biphenyl (RbBp) ion pair, of which the anion contains only carbon and hydrogen atoms. The crystals prepared from tetraglyme ($CH_3O(CH_2CH_2O)_4CH_3$) have the composition RbBp·2Ttg (Ttg = tetraglyme) and belong to the category of solvent-separated ion pairs, since the Rb cation is completely surrounded by two tetraglyme molecules and coordinated to the tetraglymes through the ten oxygen atoms.

The magnetic properties of the crystals have been investigated by ESR, NMR, and with the foner vibrating sample magnetometer. The ESR spectrum consists of one single exchange-narrowed line. Its line width depends on the orientation of the magnetic field with respect to the crystal axes. With the theory of Anderson and Weiss[7] and Van Vleck,[8] a satisfactory explanation could be given for this line-width variation. Susceptibility measurements revealed an antiferromagnetic coupling in the crystals. With the aid of a singlet–triplet model, a satisfactory account could be given for the temperature dependence of the susceptibility.

Experimental Section

Preparation of the Crystals. Solutions (1.0 M) of the RbBp salt were prepared under high vacuum using standard techniques.[2] From these solutions, single crystals were obtained by slowly cooling down the solutions to about 10°C, 1°C/h. The crystals were mounted in thin glass capillaries in a He atmosphere using a home-built glovebox since the crystals are sensitive to air and moisture. In view of the low melting point (45°C) of the crystals, these manipulations were carried out at a temperature of about −20°C.

Structure Determination. $Rb^+[CH_3O(CH_2CH_2O)_4CH_3]_2C_{12}H_{10}^-$ unit cell dimensions and intensities were obtained from a crystal of approximate dimensions 0.54 × 0.18 × 0.20 mm at 100 K, with a computer-controlled Nonius CAD 3 diffractometer (Zr-filtered Mo Kα radiation, λ 0.71069 Å, θ–2θ scan). Systematic absences are hkl for $h + k$ odd, $h0l$ for l odd and $0k0$ for k odd, these are consistent with the space groups $C2/c$ and Cc. The structure was successfully refined in the centrosymmetric space group $C2/c$. Unit cell dimensions are: a = 30.68 (3), b = 9.79 (1), c = 23.71 (2) Å, β = 103.34 (6)°, V = 6909 Å^3, d_x = 1.31 g/cm^3, Z = 8. Linear absorption coefficient μ = 15.7 cm^{-1}.

Of the 6097 symmetry-independent reflections up to θ = 25°, 3573 reflections were observed above background [$I > 3\sigma_c(I)$, $\sigma_c(I)$ derived from counting statistics]. The observed intensities were corrected for Lorentz and polarization effects and absorption. The latter corrections were calculated according to the Busing and

Table I. Final Positional Parameters for the Nonhydrogen Atoms with Standard Deviation in Parentheses

	x	y	z
Rb	0.12828 (2)	0.26209 (6)	0.11064 (2)
		Tetraglyme I	
C(13)	0.0752 (3)	−0.0103 (8)	−0.0125 (3)
O(1)	0.0622 (2)	0.1099 (5)	0.0142 (2)
C(14)	0.0327 (3)	0.1921 (7)	−0.0283 (3)
C(15)	0.0210 (2)	0.3171 (8)	0.0025 (3)
O(2)	0.0577 (2)	0.4028 (5)	0.0262 (2)
C(16)	0.0744 (3)	0.4764 (8)	−0.0168 (3)
C(17)	0.1102 (2)	0.5730 (7)	0.0136 (3)
O(3)	0.1492 (1)	0.4941 (4)	0.0410 (2)
C(18)	0.1861 (3)	0.5799 (7)	0.0642 (3)
C(19)	0.2260 (2)	0.4907 (8)	0.0910 (3)
O(4)	0.2178 (1)	0.4348 (5)	0.1431 (2)
C(20)	0.2513 (2)	0.3374 (8)	0.1694 (4)
C(21)	0.2427 (2)	0.2917 (7)	0.2258 (3)
O(5)	0.2008 (2)	0.2211 (4)	0.2159 (2)
C(22)	0.1897 (3)	0.1887 (8)	0.2694 (3)
		Tetraglyme II	
C(23)	0.1461 (2)	0.5421 (7)	0.2213 (3)
O(6)	0.1126 (2)	0.5291 (5)	0.1672 (2)
C(24)	0.0675 (2)	0.5368 (7)	0.1738 (3)
C(25)	0.0538 (2)	0.4167 (7)	0.2052 (3)
O(7)	0.0538 (1)	0.2968 (4)	0.1704 (2)
C(26)	0.0383 (2)	0.1815 (7)	0.1970 (3)
C(27)	0.0457 (2)	0.0557 (7)	0.1656 (3)
O(8)	0.0931 (1)	0.0376 (4)	0.1726 (2)
C(28)	0.1045 (2)	−0.1019 (7)	0.1634 (3)
C(29)	0.1535 (2)	−0.1074 (6)	0.1631 (3)
O(9)	0.1592 (1)	−0.0428 (5)	0.1112 (2)
C(30)	0.2047 (2)	−0.0373 (6)	0.1077 (3)
C(31)	0.2057 (2)	0.0138 (7)	0.0479 (3)
O(10)	0.1904 (1)	0.1525 (4)	0.0432 (2)
C(32)	0.1826 (2)	0.1992 (7)	−0.0154 (3)
		Biphenyl Anion	
C(1)	0.1217 (2)	0.4674 (6)	0.3666 (3)
C(2)	0.0934 (2)	0.3487 (7)	0.3611 (3)
C(3)	0.1098 (2)	0.2200 (7)	0.3776 (3)
C(4)	0.1559 (2)	0.1987 (7)	0.4021 (3)
C(5)	0.1842 (2)	0.3125 (7)	0.4084 (3)
C(6)	0.1682 (2)	0.4426 (7)	0.3910 (3)
C(7)	0.1044 (2)	0.6017 (6)	0.3493 (2)
C(8)	0.0573 (2)	0.6284 (6)	0.3331 (3)
C(9)	0.0406 (2)	0.7569 (7)	0.3159 (3)
C(10)	0.0690 (2)	0.8678 (7)	0.3132 (3)
C(11)	0.1155 (2)	0.8435 (7)	0.3299 (3)
C(12)	0.1325 (2)	0.7151 (6)	0.3474 (3)

Levy[9] scheme; 4 × 4 × 4 volume fragments and seven bounding planes were taken into account. The unobserved reflections were not used.

The structure was solved by a combination of Patterson and direct method techniques. From a Patterson synthesis, the position of the rubidium cation was determined (Table I). The remaining light atom structure was then solved by direct methods from the known heavy-atom position using the automatic program DIRDIF-B.[10] The atomic coordinates and the anisotropic thermal parameters (Table II) of all nonhydrogen atoms were refined by least-squares methods. The function that was minimized was $\Sigma w[|F_o| - K|F_c|]^2$, with $w^{-1} = \sigma(F_o)^2 + (0.05|F_o|)^2$. The hydrogen atoms were placed at calculated positions. Hydrogen atoms of the biphenyl anion were placed on the bisector of the C-CH-C angle (CH is the carbon atom to which the hydrogen atom is attached) at a C-H distance of 1.084 Å. Hydrogen atoms attached to the end carbon atoms of the tetraglyme molecules were placed staggered with respect to the tetraglyme chain at a C-H distance of 1.101 Å and H-C-H angles of 109.47°. The remaining hydrogen atoms of the tetraglyme molecules were placed in the plane bisecting the O-CH-C angle, at a C-H distance of 1.073 Å and with an H-C-H angle of 109.47°. All hydrogen atoms were included in the structure factor calculations with a temperature factor equal to the isotropic equivalent of their parent carbon atoms, but they were not refined. Final conventional R value is 0.054 for all 3573 observed reflections.[11] The atomic scattering factors used were those for Rb^+ (corrected for anomalous scattering $\Delta f'$), O, C, and H as given in the "International Tables for X-ray Crystallography".[12] If no standard deviations are given explicitly, the standard deviation is one in the last digit.

Magnetic Measurements. The ESR experiments were performed on a Varian E12 spectrometer at X band (9.3 GHz) as well as at Q band (35 GHz) and on an AEG 20 XT spectrometer. Low temperatures were achieved with a Leybold ESR continuous flow cryostat of the Klipping type. The temperature was measured with a gold-iron chromel thermocouple and could be kept constant within 1°C. A Weisenberg camera was used for mounting the crystal along particular axes. Wide-line ^{87}Rb NMR experiments were performed on the Varian E12 spectrometer equipped with the wide-line variable frequency unit WL-210.

The dynamic relative susceptibility was measured by direct integration of the ESR absorption signal.[13] Therefore clock pulses were given to the field control unit of the flux stabilized AEG 20 XT magnet in this way producing a trapezoid field modulation with a modulation frequency of 0.05 Hz. The absorption intensity was corrected for eventual baseline drift.

Results and Discussion

Crystal Structure. The molecular structure (Figure 1) can be described as a solvent-separated ion pair, consisting of a rubidium cation coordinated to two tetraglyme molecules and a biphenyl anion. The ten coordinating oxygen atoms of the two glymes lie on a sphere around the rubidium ion as can be seen in the stereoscopic picture (Figure 2). The average rubidium-oxygen bond length of 3.01 (3) Å (Table III) resembles the average rubidium-oxygen bond length in dirubidium cyclooctatetraene diglyme (3.02 (15) Å).[5] As can be seen from the difference of the average rubidium-oxygen distance and the van der Waals radius of oxygen (1.40 Å),[14] the van der Waals radius of the rubidium ion (1.60 (3) Å) is slightly larger than its ionic radius (1.47 Å).[14] Bond lengths and bond angles of the biphenyl anion are shown in Figure 3.

Although the phenyl rings are planar within experimental error (maximum deviation of the least-squares plane is 0.008 Å), the dihedral angle between the two rings turns out to be 9.4°. As neutral biphenyl is reported to be flat in the solid state,[15,16] the explanation of this dihedral angle might be found in a change of the bond order going from neutral biphenyl to the monoanion. The values in parentheses given in Figure 4 denote the calculated bond lengths (R) using the relation[17] $R = 1.517 - 0.18P$, where P gives the bond order. The latter was calculated with the SCF-MO method, assuming planar structures. The shortened distance between the two phenyl rings in the monoanion as compared with the neutral molecule increases the repulsion between the ortho hydrogen atoms and may therefore cause the change in the dihedral angle. The ortho hydrogen repulsion expresses itself furthermore in the C(8)-C(7)-C(12) and C(2)-C(1)-C(6) bond angles, which are significantly smaller than 120°.

The direction of rotation of the phenyl rings may be caused by the remarkable short intermolecular distance between the two biphenyl molecules which are related by the twofold rotation axis. The shortest distance of 3.50 Å between the carbon atoms C(9) and C(9′) is less than twice the van der Waals radius of carbon which is 1.85 Å.[14] The distance between the centers of these symmetry related molecules is 7.58 Å. This is much shorter than the distance to the next nearest neighbors (9.79 Å) which can be found by a translation along the b axis.

Magnetic Properties. Figure 5 presents the angular dependence of the ESR line width at room temperature of a single crystal of RbBp·2Ttg at X-band frequency. The magnetic field is parallel to the ac plane, for which orientation

Table II. Anisotropic Thermal Parameters for the Nonhydrogen Atoms with Standard Deviation in Parentheses (in Å²)

	U_{11}	U_{22}	U_{33}	U_{12}	U_{13}	U_{23}
Rb	0.0199 (4)	0.0208 (4)	0.0180 (4)	0.0004 (3)	0.0016 (2)	0.0002 (3)
			Tetraglyme I			
C(13)	0.034 (5)	0.052 (5)	0.038 (5)	0.003 (4)	0.000 (4)	−0.014 (4)
O(1)	0.036 (3)	0.036 (3)	0.022 (3)	0.006 (2)	0.000 (2)	−0.005 (2)
C(14)	0.038 (5)	0.037 (4)	0.024 (4)	0.006 (3)	−0.008 (3)	−0.003 (3)
C(15)	0.032 (5)	0.044 (5)	0.033 (4)	0.012 (3)	−0.006 (3)	0.004 (3)
O(2)	0.026 (3)	0.038 (3)	0.028 (3)	0.005 (2)	0.004 (2)	0.003 (2)
C(16)	0.043 (5)	0.041 (5)	0.020 (4)	0.013 (3)	0.004 (3)	0.005 (3)
C(17)	0.044 (5)	0.030 (4)	0.024 (4)	0.006 (3)	0.010 (3)	0.007 (3)
O(3)	0.034 (3)	0.023 (3)	0.026 (3)	−0.002 (2)	0.004 (2)	0.001 (2)
C(18)	0.044 (5)	0.032 (4)	0.037 (4)	−0.013 (4)	0.010 (4)	0.001 (3)
C(19)	0.032 (5)	0.050 (5)	0.038 (4)	−0.021 (4)	0.014 (4)	−0.009 (4)
O(4)	0.028 (3)	0.041 (3)	0.031 (3)	0.000 (2)	0.011 (2)	−0.009 (2)
C(20)	0.016 (4)	0.043 (5)	0.065 (6)	0.000 (3)	0.001 (4)	−0.022 (4)
C(21)	0.031 (4)	0.041 (5)	0.039 (4)	0.005 (3)	−0.017 (3)	−0.005 (3)
O(5)	0.036 (3)	0.032 (3)	0.024 (2)	−0.003 (2)	−0.007 (2)	−0.003 (2)
C(22)	0.080 (7)	0.039 (5)	0.021 (4)	0.004 (4)	0.000 (4)	−0.001 (3)
			Tetraglyme II			
C(23)	0.032 (4)	0.037 (4)	0.020 (3)	0.003 (3)	0.004 (3)	0.000 (3)
O(6)	0.037 (3)	0.035 (3)	0.023 (2)	0.000 (2)	0.006 (2)	−0.001 (2)
C(24)	0.028 (4)	0.031 (4)	0.034 (4)	0.003 (3)	0.011 (3)	−0.001 (3)
C(25)	0.030 (4)	0.029 (4)	0.028 (4)	0.002 (3)	0.009 (3)	−0.002 (3)
O(7)	0.031 (3)	0.028 (3)	0.022 (2)	0.000 (2)	0.007 (2)	0.004 (2)
C(26)	0.023 (4)	0.033 (4)	0.032 (4)	−0.004 (3)	0.012 (3)	0.002 (3)
C(27)	0.025 (4)	0.040 (5)	0.035 (4)	0.010 (3)	0.008 (3)	−0.002 (3)
O(8)	0.024 (3)	0.028 (3)	0.033 (3)	0.002 (2)	0.005 (2)	0.001 (2)
C(28)	0.037 (5)	0.022 (4)	0.041 (4)	0.000 (3)	0.011 (3)	0.002 (3)
C(29)	0.044 (5)	0.024 (4)	0.027 (4)	0.006 (3)	0.009 (3)	0.006 (3)
O(9)	0.027 (3)	0.036 (3)	0.023 (2)	0.002 (2)	0.002 (2)	0.002 (2)
C(30)	0.026 (4)	0.025 (4)	0.027 (4)	0.010 (3)	0.001 (3)	−0.002 (3)
C(31)	0.025 (4)	0.030 (4)	0.031 (4)	0.005 (3)	0.005 (3)	−0.003 (3)
O(10)	0.030 (3)	0.027 (3)	0.022 (2)	0.005 (2)	0.003 (2)	−0.002 (2)
C(32)	0.036 (4)	0.035 (4)	0.018 (3)	−0.001 (3)	0.005 (3)	0.001 (3)
			Biphenyl Anion			
C(1)	0.027 (4)	0.027 (4)	0.015 (3)	−0.001 (3)	0.007 (3)	−0.001 (3)
C(2)	0.033 (4)	0.033 (4)	0.015 (3)	−0.005 (3)	−0.002 (3)	0.000 (3)
C(3)	0.034 (4)	0.035 (4)	0.021 (3)	−0.004 (3)	−0.007 (3)	−0.002 (3)
C(4)	0.034 (4)	0.030 (4)	0.026 (4)	0.001 (3)	0.009 (3)	0.004 (3)
C(5)	0.025 (4)	0.037 (4)	0.018 (3)	0.007 (3)	0.004 (3)	0.001 (3)
C(6)	0.024 (4)	0.029 (4)	0.022 (3)	−0.003 (3)	0.005 (3)	−0.005 (3)
C(7)	0.025 (4)	0.024 (4)	0.013 (3)	−0.003 (3)	0.001 (3)	−0.002 (3)
C(8)	0.023 (4)	0.026 (4)	0.022 (4)	0.003 (3)	−0.001 (3)	0.001 (3)
C(9)	0.029 (4)	0.039 (4)	0.021 (3)	0.004 (4)	−0.002 (3)	−0.005 (3)
C(10)	0.042 (5)	0.032 (4)	0.022 (4)	0.001 (3)	0.003 (3)	0.000 (3)
C(11)	0.033 (4)	0.032 (4)	0.027 (4)	−0.003 (3)	0.005 (3)	−0.004 (3)
C(12)	0.024 (4)	0.023 (4)	0.019 (3)	−0.002 (3)	0.003 (3)	−0.001 (2)

Table III. Bond Distances (in Å) and Angles (in Degrees) for the Rubidium Tetraglyme Part of $Rb^+[CH_3O(CH_2CH_2O)_4CH_3]_2C_{12}H_{10}^-$ [a]

	Smallest value	Largest value	Average value
Rb–O	2.928	3.154	3.015
	Tetraglyme Molecules		
C–O	1.410	1.452	1.430
C–C	1.484	1.517	1.501
C–O–C	110.1	113.7	111.7
O–C–C	107.3	114.7	109.1

[a] Only minimal, maximal, and average values are given for corresponding bonds and angles.

all biphenyl molecules are magnetically equivalent. At all observed angles, the line shape is Lorentzian. The line width (ΔH) of an exchange-narrowed line can be described by a formula, derived by Anderson and Weiss[7]

$$\Delta H = \langle \Delta\omega^2 \rangle / \omega_e$$

where $\langle \Delta\omega^2 \rangle$ is the mean squared width or second moment in the absence of narrowing, and ω_e is an average exchange frequency. To find an expression for the second moment, van Vleck[8] introduced a truncated Hamiltonian, which means that all off-diagonal parts in the magnetic dipolar interaction between the unpaired electrons are neglected. It reads

$$\mathcal{H}_{\text{trunc}} = g\beta H_0 \sum_j S_{z_j} + \tfrac{1}{2} g^2\beta^2 \sum_{j>k} r_{jk}^{-3}(3\cos^2\theta_{jk} - 1)[\bar{S}_j \cdot \bar{S}_k - 3S_{z_j}S_{z_k}] - 2J\sum_{j>k} \bar{S}_j \cdot \bar{S}_k$$

where r_{jk} gives the distance between the spins j and k and θ_{jk} gives the angle between the direction of r_{jk} and the magnetic field. The spins are thought to be located in the centers of the biphenyl molecules. Neglecting the off-diagonal elements in the Hamiltonian is allowed only if $(\omega_0\tau_e)^2 \gg 1$, where ω_0 is the Larmor precession frequency and τ_e the electron correlation time ($\tau_e = \omega_e^{-1}$). As will be shown later, this condition is satisfied in our case. With the aid of $\mathcal{H}_{\text{trunc}}$, van Vleck[8] calculated for the second moment

$$\langle \Delta\omega^2 \rangle = \tfrac{3}{4} S(S+1)\gamma^4\hbar^2 \sum_k r_{jk}^{-6}(3\cos^2\theta_{jk} - 1)^2$$

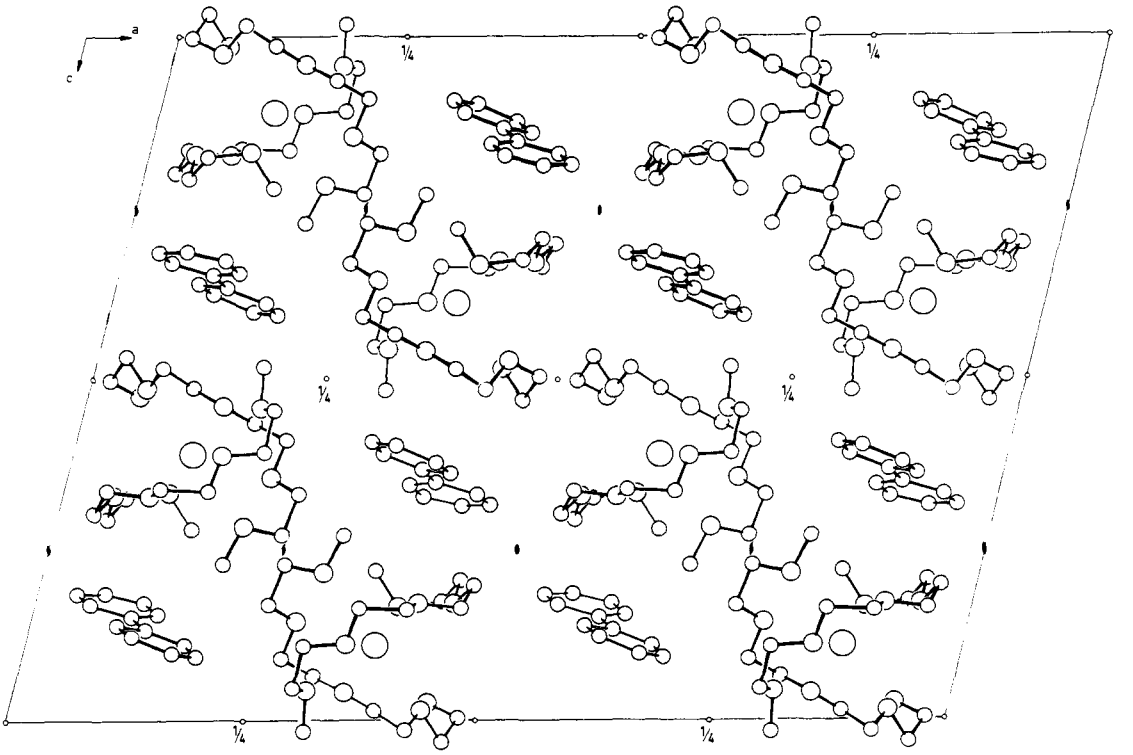

Figure 1. The *ac* projection of the unit cell of $Rb^+[CH_3O(CH_2CH_2O)_4CH_3]_2C_{12}H_{10}^-$. The symmetry elements are indicated in the picture. The circles of decreasing size are respectively: Rb, O, and C.

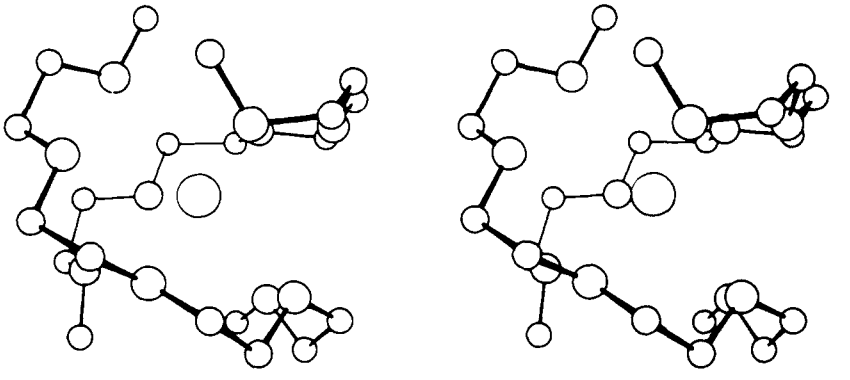

Figure 2. A stereoscopic view of the solvation of rubidium by two tetraglyme molecules.

Through the r_{jk}^{-6} dependence, the largest contribution to the second moment arises from the nearest neighbor spins, which are at an average distance of 7.58 Å. The next nearest spins are at average distances of 9.79 Å; their contribution to the second moment in the *ac* plane is angular independent, because the angle θ is 90°. The contribution of further removed spins is almost angular independent. In Figure 5 the dashed line represents the $(3\cos^2\theta - 1)^2$ behavior of nearest neighbor spins, which has been added to an angular independent part of 1.24 G due to the contribution of the other spins. As can be seen from the figure, the experimental line widths measured in the *ac* plane follow this behavior rather closely; the minima and maxima are found at the correct angles.

The neglect of the off-diagonal elements in the complete Hamiltonian can be verified by calculating τ_c from the line width at a certain angle and from the calculated second moment. It was found that $\tau_c = 3 \times 10^{-10}$ s, which renders $(\omega_0\tau_c)^2 \gg 1$ both at X- and Q-band frequencies. In agreement with this no relevant changes were observed in measuring the line width at Q band instead of at X band (absence of "10/3 effect").[7]

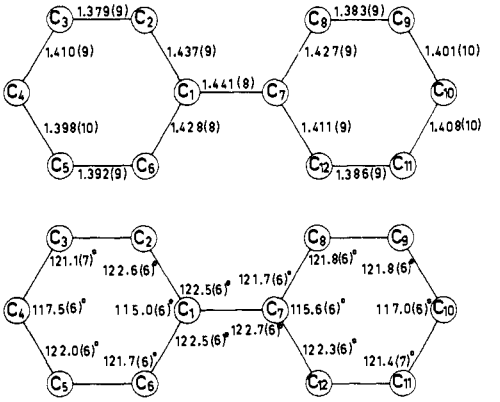

Figure 3. Bond distances (in Å) and angles (in degrees) in the biphenyl anion with standard deviation in parentheses.

The experimental data on the relative paramagnetic susceptibility are presented in Figure 5. It is clear that an antiferromagnetic coupling exists in the crystal. At 15 K a maximum is reached in the susceptibility. If coupling exists only

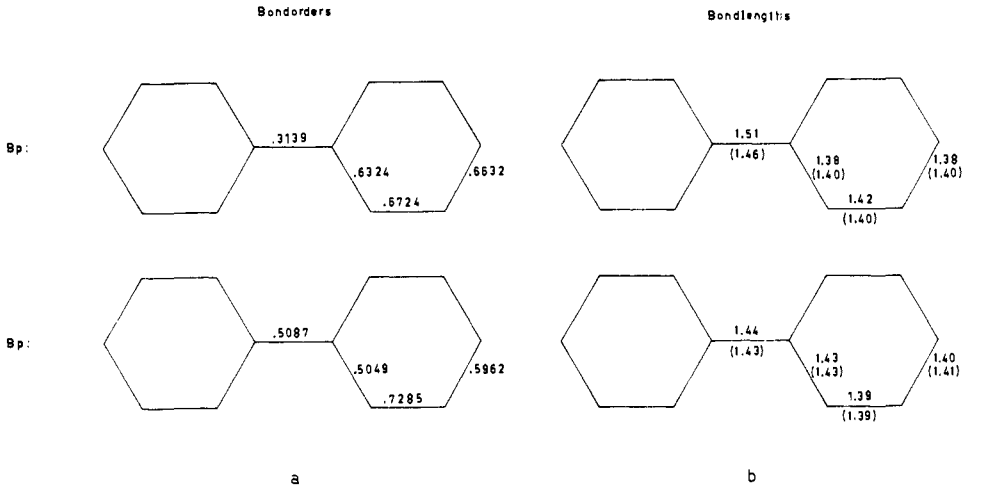

Figure 4. (a) Bond orders in Bp and Bp^- from SCF molecular orbital calculation assuming planar structures. (b) Average experimental and calculated[16] bond lengths in Bp and Bp^-.

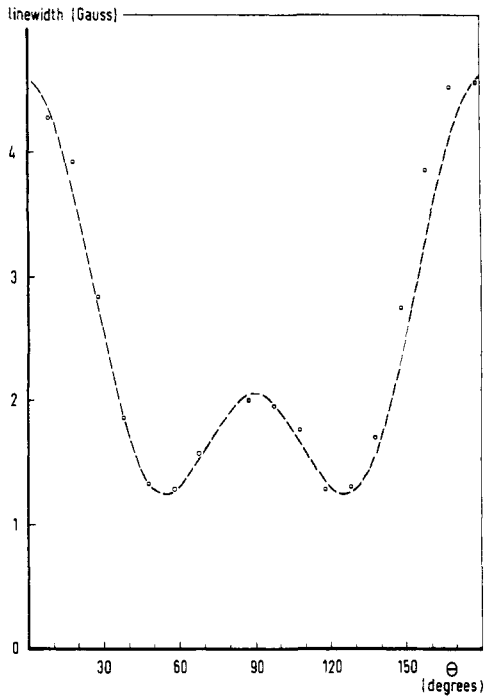

Figure 5. Angular variation of the line width of a single crystal of RbBp·2Ttg. The magnetic field is parallel to the *ac* plane.

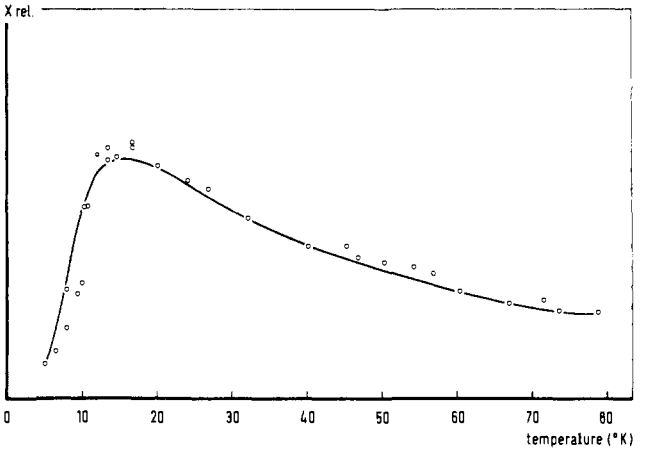

Figure 6. Relative paramagnetic susceptibility of a single crystal of RbBp·2Ttg. Solid curve: singlet-triplet model.

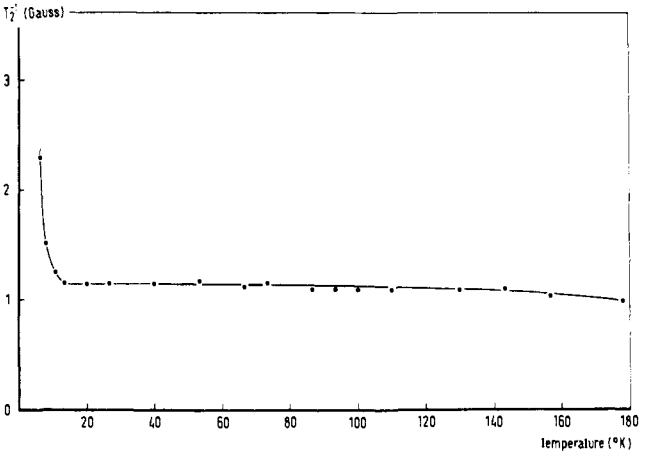

Figure 7. The temperature dependence of the line width of a single crystal of RbBp·2Ttg in an arbitrary orientation.

between nearest neighbor spins, singlet ground-state dimers can be distinguished in the crystal, each having a triplet state lying at an energy $\delta = -2J$ above this ground state (according to definition J is negative for antiferromagnetic coupling). The susceptibility based on this singlet-triplet model is then given by the well-known expression

$$\chi = \frac{4Ng^2\beta^2}{kT}\frac{1}{3 + e^{\delta/kT}}$$

where N is the number of paramagnetic molecules. Using this formula the susceptibility data can be fitted rather well (Figure 6). From the maximum in the curve one derives that $\delta/k = 2J/k = 24$ K since $\delta = 1.61kT_{max}$, where T_{max} is the temperature at which the susceptibility reaches its maximum. This temperature has been confirmed by a susceptibility measurement by means of the foner vibrating sample magnetometer.

Above 30 K the susceptibility follows the Curie-Weiss law, with a negative Weiss constant, $\theta = -7$ K. This value can be used to check the derived value of J, because there exist relationships between θ and J. For instance, the Weiss molecular field approximation gives a relation

$$\theta = [2zJS(S + 1)]/3k$$

where z is the number of nearest neighbor spins. With $z = 1$ and $\theta = -7$ K, one finds for $2J/k = -28$ K in good agreement with the value cited above.

Figure 7 shows the line width as a function of tempera-

ture. The line shape is Lorentzian at all observed temperatures. The increased line width at temperatures below T = 15 K is an additional indication of magnetic ordering at low temperatures,[18] leading to a decrease in exchange frequency.

^{87}Rb NMR. On a polycrystalline sample of RbBp·2Ttg, a ^{87}Rb NMR experiment has been carried out. A single resonance line was observed with a derivative line width of 8 G. This line was not shifted with respect to the ^{87}Rb resonance line of a RbCl solution in water. These observations are in agreement with the crystallographic structure, where it was found that the Rb cation is almost spherically surrounded by two tetraglyme molecules. Such a structure will lead to a small electric field gradient and a zero spin density at the Rb nucleus, giving rise to a single, unshifted resonance line.

Conclusion

In conclusion the RbBp·2Ttg crystal can be described as a solvent-separated ion pair. In this regard, it substantiates the conclusions drawn by Canters and de Boer[19] for the RbBp ion-pair structures in solvents of high solvating power. From the shift and the line width of the Rb resonance line, it was concluded that solvent-separated ion pairs existed in the solution, as is now also borne out in the solid state.

Acknowledgments. One of the authors (J.J.M.) enjoyed the helpful discussions with Dr. J. M. Trooster about the making of the sweep unit for the susceptibility measurements. He is also very thankful to Mr. C. J. Beers for his skillful assistance in carrying out the foner susceptibility experiments. Part of this work (Th.v.d.H) has been carried out under the auspices of FOMRE with financial support of the Netherlands Organization for the Advancement of Pure Research (ZWO).

Supplementary Material Available: Structure factor tables (34 pages). Ordering information is given on any current masthead page.

References and Notes

(1) M. Szwarc, "Ion and Ion Pairs in Organic Reactions", Vol. 1, Wiley-Interscience, New York, N.Y., 1972; E. S. Petrov, M. I. Terekhova, and A. I. Shatenshtein, *Russ. Chem. Rev.*, **42**, 713 (1973); N. L. Holy, *Chem. Rev.*, **74**, 243 (1974).
(2) G. W. Canters, A. A. K. Klaassen, and E. de Boer, *J. Phys. Chem.*, **74**, 3299 (1970).
(3) (a) J. J. Brooks and G. D. Stucky, *J. Am. Chem. Soc.*, **94**, 7333 (1972); (b) J. J. Brooks, W. Rhine, and G. D. Stucky, *ibid.*, **94**, 7339 (1972); (c) *ibid.*, **94**, 7346 (1972).
(4) S. Z. Goldberg, K. N. Raymond, C. A. Harmon, and D. H. Templeton, *J. Am. Chem. Soc.*, **96**, 1348 (1974).
(5) (a) J. H. Noordik, Th. E. M. van den Hark, J. J. Mooij, and A. A. K. Klaassen, *Acta Crystallogr., Sect. B*, **30**, 833 (1974); (b) J. H. Noordik, H. M. L. Degens, and J. J. Mooij, *ibid.*, **31**, 2144 (1975).
(6) R. H. Cox, L. W. Harrison, and W. K. Austin, *J. Phys. Chem.*, **77**, 200 (1973).
(7) P. W. Anderson and P. R. Weiss, *Rev. Mod. Phys.*, **25**, 269 (1953).
(8) J. H. van Vleck, *Phys. Rev.*, **74**, 1168 (1948).
(9) W. R. Busing and H. A. Levy, *Acta Crystallogr.*, **10**, 180 (1957).
(10) R. O. Gould, Th. E. M. van den Hark, and P. T. Beurskens, *Acta Crystallogr., Sect. A*, **31**, 813 (1975).
(11) Observed and calculated structure factors are available from the authors.
(12) "International Tables for X-ray Crystallography", Vol. 3, Kynoch Press, Birmingham, 1962.
(13) G. T. Pott, Thesis ("Mollonic Lattices"), Groningen, 1966, pp 19–24.
(14) "Handbook of Chemistry and Physics", 49th ed, Chemical Rubber Publishing Co., Cleveland, Ohio, 1968.
(15) J. Trotter, *Acta Crystallogr.*, **14**, 1135 (1961).
(16) A. Hargreaves and S. H. Rizvi, *Acta Crystallogr.*, **15**, 365 (1962).
(17) C. A. Coulson and A. Golebiewski, *Proc. Phys. Soc., London*, **78**, 1310 (1961).
(18) J. Yamauchi, T. Fujito, E. Ando, H. Nishiguchi, and Y. Deguchi, *J. Phys. Soc. Jpn.*, **25**, 1558 (1968).
(19) G. W. Canters and E. de Boer, *Mol. Phys.*, **26**, 1185 (1973).

Magnetic Investigation of the Electronic Structure of Hexakis(pyridine *N*-oxide)cobalt(II) Perchlorate

R. L. Carlin,* C. J. O'Connor, and S. N. Bhatia

Contribution from the Department of Chemistry, University of Illinois at Chicago Circle, Chicago, Illinois 60680. *Received May 15, 1975*

Abstract: Although the CoO_6 coordination sphere of $[Co(C_5H_5NO)_6](ClO_4)_2$ is perfectly octahedral, it is shown from a magnetic study at low temperatures that the cobalt ion suffers a large electronic or crystal field distortion. The g values are $g_\parallel = 2.26 \pm 0.01$ and $g_\perp = 4.77 \pm 0.01$ from EPR measurements of cobalt doped into $[Zn(C_5H_5NO)_6](ClO_4)_2$, while the parameters $g_\parallel = 2.49 \pm 0.05$, $g_\perp = 4.70 \pm 0.05$ were obtained from susceptibility studies on the pure cobalt compound. The compound obeys the Curie–Weiss law, 1.5–20 K, with $\theta_\parallel = -0.28 \pm 0.05$ K, $\theta_\perp = -0.52 \pm 0.05$ K. The g values and TIP terms also allow an estimate of the position of the low-lying components of the $^4T_1(F)$ state.

The recent discovery[1-3] that $[Zn(C_5H_5NO)_6](ClO_4)_2$, where C_5H_5NO is pyridine *N*-oxide, assumes a rhombohedral crystal structure with but one molecule in the unit cell, makes this lattice an attractive one for a variety of physical studies. This molecule, as well as its isomorphous manganese, cobalt, and nickel congeners, has been known for some time[4] and although an extensive transition metal chemistry of aromatic *N*-oxides has since developed,[5] there have been relatively few single-crystal studies. The EPR spectrum of manganese(II) doped into the zinc lattice was recently reported,[1] and, although the molecules are geometrically undistorted,[2,3] a rather large zero-field splitting was observed. It was reported[6] that no EPR spectrum was observed for powdered samples of $[Ni(C_5H_5NO)_6](ClO_4)_2$ at room temperature, and we have found that no such spectrum is observable at X-band in doped $[Ni,Zn(C_5H_5NO)_6](ClO_4)_2$ single crystals even at helium temperatures. These results are consistent with a large zero-field splitting also occurring for the nickel system.

We have chosen the cobalt(II) ion as a probe for continuing our studies of crystal field effects in this lattice. The theory of the electronic structure of the hexaaquocobalt(II) ion is particularly well developed[7-10] and one expects that the metal–oxygen bond in the pyridine *N*-oxide complexes will be sufficiently similar to allow this theory to be used here. EPR studies at helium temperatures of divalent cobalt